

Simulation of Hysteresis and Eddy Current Effects in a Power Transformer

W. Chandrasena¹, P.G. McLaren², U.D. Annakkage¹,
R.P. Jayasinghe³, D. Muthumuni³, and E. Dirks¹

(1) Department of Electrical and Computer Engineering, University of Manitoba, Winnipeg, Manitoba, Canada R3T5V6 (e-mail: waruna@cc.umanitoba.ca, annakag@cc.umanitoba.ca, dirks@cc.umanitoba.ca), (2) The Center for Advanced Power Systems, Florida State University, Tallahassee, Florida 32310, USA (e-mail: mclaren@caps.fsu.edu), (3) Manitoba HVDC Research Centre, Winnipeg, Manitoba, Canada R3J3W1 (e-mail: jayas@hvdc.ca, dharshana@hvdc.ca)

Abstract— This paper presents a simulation algorithm to simulate the hysteresis characteristics in the core of a power transformer. The algorithm is based on the Jiles-Atherton phenomenological model of a ferromagnetic material. The new transformer model is capable of producing a close representation of the transformer magnetizing current. Comparisons are made between recorded and simulated waveforms using a single phase distribution transformer. A good agreement is achieved between recorded and simulated data.

Keywords - eddy currents, hysteresis, losses, power transformers, simulation

I. INTRODUCTION

A bibliographic review of the hysteresis models presented during the past three decades is given in [1]. Many of these attempts are curve fits, which ignore the underlying physics of the material behavior. At the other extreme, micromagnetic methods consider all known energies on a very small scale and find the domain configuration that gives the minimum energy. In general intermediate solutions models, which can relate micro-structural parameters to the macroscopic responses of the material to outside fields are more suitable for time domain simulations [2]. Four magnetization models are now considered as classical. They are the Stoner-Wolfarth model, the Jiles-Atherton model [3], the Globus model, and the Preisach model. The methods each model uses to simulate the magnetization mechanisms, their advantages and disadvantages are discussed in [2].

This paper shows how the Jiles-Atherton (JA) phenomenological model of a ferromagnetic material is incorporated into a subroutine for use in an electromagnetic transient simulation program to simulate a power transformer. This has been used in [4] in the simulation of current transformers, and it has been shown that the hysteresis model based on the JA theory accurately represents the remanence flux and minor loops in the transformer cores. The new model also includes the frequency dependent losses. The eddy current effects are incorporated into the algorithm before the transformer inductance matrix is calculated. Thus, the calculated value of the saturation current injected across each winding also contains the effects of eddy currents. Therefore this method is useful in the simulation of multi-winding transformers.

Modeling of transformers of varying complexity have been implemented in electromagnetic transient simulation programs to simulate the transient behavior [5]-[11]. The correct representation of the hysteresis loop is important so that it handles long term remanence and recoil loops. In short time simulations the piecewise linear solutions of saturation can give the impression that they handle remanence because the system time constants maintain the magnetization over several hundreds of milliseconds. However, over time scales of seconds the flux will decay to zero. It is usually possible to initialize the remanence in a typical transformer model, however it requires outside intervention whereas our method presented in this paper will do it automatically.

The electromagnetic transient simulation software PSCAD/EMTDC has multi-limb transformer models based on a unified magnetic equivalent circuit (UMEC) [10]. In this paper we have used the transformer core model presented in [10] as the basis of this work and describes how the Jiles Atherton theory can be incorporated into a simulation algorithm of a power transformer in an electromagnetic transient simulation program.

II. REVIEW OF THE TRANSFORMER CORE MODEL

A brief review of the transformer core model described in [10] is presented in this section, and it explains how the saturation is modeled in this core model in EMTDC. The core model of a single phase two winding transformer uses the magnetic circuit shown in Fig.1. The magnetic equivalent circuit of the transformer is given in Fig.2.

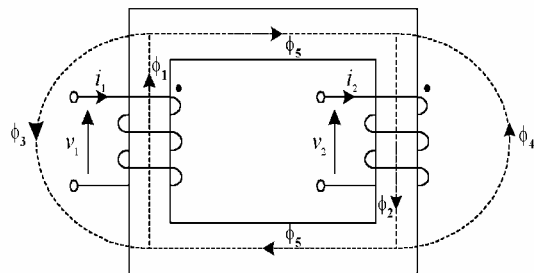


Fig. 1. Single phase transformer flux paths, unified magnetic paths

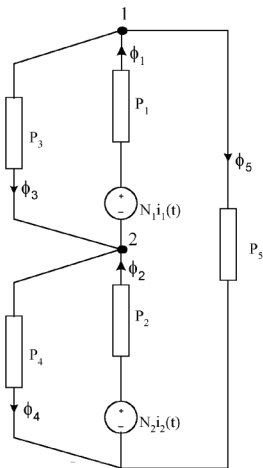


Fig. 2. Magnetic equivalent circuit for single phase two winding transformer model

The branches of magnetic equivalent circuit represent the assumed paths of flux, i.e. the transformer winding limbs (ϕ_1 and ϕ_2), the leakage (ϕ_3 and ϕ_4), and the yokes (ϕ_5). The two winding transformer has two *MMF* sources, $N_1 i_1(t)$ and $N_2 i_2(t)$ to represent individual windings. P_1 and P_2 represent the permeance of the transformer winding limbs and P_5 represents the permeance of the transformer yokes. P_3 and P_4 represent the permeances of the leakage paths.

In an electromagnetic transient simulation program, the representation of a transformer begins with the calculation of the transformer inductance matrix (L). In this model, the transformer inductance matrix has been derived using the magnetic equivalent circuit in Fig.2. The following section describes how the transformer inductance matrix (L) is calculated using this magnetic equivalent circuit.

A. Calculation of the transformer inductance matrix

The description of the single phase two winding transformer presented in the previous section is considered. The branch node connection matrix $[A]$ is used to define the sum of the flux at each node. i.e. the total flux at each node must add up to zero. Therefore, this representation includes details of the configuration of the transformer core; i.e. three phase three limb, three phase five limb etc. Thus the calculated transformer inductance matrix is dependent on the magnetic equivalent circuit of a given transformer.

The *MMF* across each branch of the magnetic circuit has been written in the vector form as in (1), where θ is the vector of branch *MMF*s, N is a diagonal matrix containing the number of turns in each winding, R is the diagonal matrix containing reluctance of each branch, ϕ is the vector of branch flux. Using these equations, the relationship between the flux and current has been obtained as in (2). $[P]$ is the diagonal matrix containing permeance of each branch.

$$\theta = [N]i - [R]\phi \quad (1)$$

$$\phi = [M][N]i \quad (2)$$

$$[M] = [P] - [P][A]([A]^T[P][A])^{-1}[A]^T[P] \quad (3)$$

The magnitude of the current injected across each winding is found by using the vector of branch flux (ϕ), that is partitioned into a set that contains the branches associated with each transformer winding. Therefore (2) becomes (4), where ϕ_s is the vector containing the winding flux ϕ_1 and ϕ_2 , i_s is the vector containing the winding current i_{s1} and i_{s2} , $[N_{ss}]$ is a diagonal matrix of winding turns N_1 and N_2 , and $[M_{ss}]$ is a square permeance matrix.

$$\phi_s = [M_{ss}][N_{ss}]i_s \quad (4)$$

A further development to this transformer model has been presented [11], in which the necessity to input detailed core data such as the lengths (l) and the cross-sectional areas (A) of each limb, and the actual number of turns (N) in each winding has been eliminated. In this method, instead of calculating the transformer inductance matrix using the actual values of N , A , and l , an equivalent inductance matrix is calculated by fixing the value of N , and calculating the appropriate values of A and l , such that the original inductance matrix is obtained.

B. The existing model

In the existing transformer model of EMTDC, the saturation is represented with a current source connected across each winding (Fig.3). A piece-wise linearly interpolated B-H characteristic curve has been used to model the saturation in the transformer core (Fig.4) [12]. In

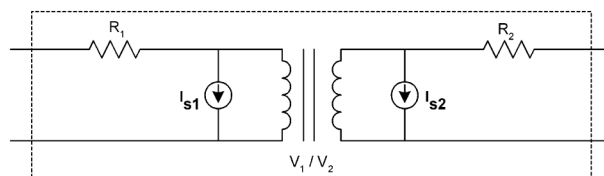


Fig. 3. Representation of saturation in EMTDC

the simulation algorithm, the differential permeability (μ_{dif}) and the magnetic field strength (H) are calculated using the piece-wise linear B-H saturation characteristic, and the flux densities (B) of winding limbs

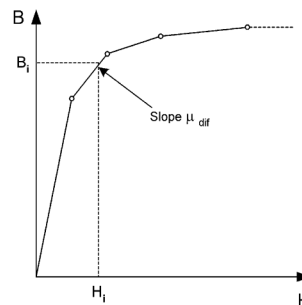


Fig. 4. Saturation curve of the existing model

and the yoke. Then the permeance of these branches are calculated to update the branch permeance matrix $[P]$. Finally, the magnitudes of the current injected for the present time step are calculated as in (5).

$$\mathbf{i}_s = \phi_s([\mathbf{M}_{ss}][\mathbf{N}_{ss}])^{-1} \quad (5)$$

III. THE NEW MODEL : INCORPORATING THE JA THEORY

The saturation model described in the previous section uses a piece-wise linear B-H characteristic to calculate the differential permeability (μ_{dif}) and the magnetic field strength (H) of the branches representing the iron core. The new model presented in this paper is based on the Jiles - Atherton theory of a ferromagnetic material. Instead of using a piece-wise linearly interpolated curve, we have incorporated the differential equations described in the JA theory to model the hysteresis characteristics of the transformer core [3]. The JA theory describes the relationship between the magnetization M and the magnetic field intensity H of the core material. However, the relationship between the flux density B , M and H is given by (6). Therefore the slope of the B-H loop can be expressed with the slope of the M-H loop as in (7). Hence, the M-H relationship described in the JA theory can be used for this purpose. Therefore in the simulation model, during each time step the slope of the M-H loop can be used in the process of updating the branch permeance matrix. Thus, the new hysteresis model is incorporated into the simulation algorithm of the power transformer.

$$B = \mu_0(M + H) \quad (6)$$

$$\mu_{dif} = \mu_0 \left(\frac{dM}{dH} + 1 \right) \quad (7)$$

The following section presents a brief overview of the JA theory and describes the expression for the slope of the M-H loop that is used in this simulation algorithm. The section V describes how these equations are incorporated into the simulation algorithm of the transformer model and the section VI presents the comparisons of simulation and measured results.

IV. JILES - ATHERTON THEORY

The Jiles - Atherton theory describes the relationship between the magnetization M and the magnetic field intensity H of a core material. The magnetization characteristic is defined by the anhysteretic magnetization function M_{an} . The anhysteretic magnetization M_{an} at a given field H_e represents the global minimum energy state, where $H_e = H + \alpha M$. H_e is the effective field, and α is a parameter which represents the inter domain-coupling. The anhysteretic magnetization M_{an} can be expressed as $M_{an} = M_{sat} f(H_e)$, where M_{sat} is the saturation magnetization and f is an arbitrary function of the effective field [3]. The function given in (8) has been used in [4] in the simulation of current transformers, where a_1 , a_2 and a_3 are constants and $a_2 > a_1$. The

same function is used to represent the anhysteretic characteristics of the core of the power transformer model, on the basis that the characteristics of the material is likely to be the same, i.e. grain oriented silicon steel.

$$M_{an} = M_{sat} \frac{a_1 H_e + H_e^2}{a_3 + a_2 H_e + H_e^2} \quad (8)$$

The JA theory leads to two components in M . The first component, irreversible magnetization, is due to pinning of the magnetic domains by discontinuities in the material structure. The second term, reversible magnetization, is due to domain wall bending in an elastic manner. The JA theory builds on these fundamental relationships and the derivative of M with respect to H can be represented as in (9). α , c and k are constants for the material being used and δ takes the value 1 or -1 based on the sign of $\frac{dH}{dt}$. This equation takes a modified form as in (10) when $(M_{an} - M)\delta$ becomes negative.

$$\frac{dM}{dH} = \left(c \frac{dM_{an}}{dH_e} + \frac{M_{an} - M}{\frac{\delta k}{\mu_0} - \frac{\alpha(M_{an} - M)}{1 - C}} \right) \frac{1}{1 - \alpha c \frac{dM_{an}}{dH_e}} \quad (9)$$

$$\frac{dM}{dH} = \left(c \frac{dM_{an}}{dH_e} \right) \frac{1}{1 - \alpha c \frac{dM_{an}}{dH_e}} \quad (10)$$

V. SIMULATION MODEL

The simulation algorithm begins with the calculation of the flux (ϕ) and the incremental flux ($\Delta\phi$) in the winding limbs using the winding voltages (v) and the values from the previous time step. Then the flux and the incremental flux in rest of the branches in the magnetic equivalent circuit are calculated.

The input to the hysteresis model are the flux (ϕ) and the incremental flux ($\Delta\phi$) of the winding limbs and the yoke. For each magnetic branch under consideration, the increment in H (ΔH) and the increment in M (ΔM) are estimated using $\Delta\phi$ as in (11) and (13) respectively. Using the estimates of ΔH and ΔM , the new values of M and H are updated as in (14) and (15). H_{old} and M_{old} are the H and M values of the previous time step. The parameter δ , which indicates the direction the magnetization is obtained from (16).

$$\Delta H = Q \Delta H_{\max} \quad \text{where } (0 \leq Q \leq 1) \quad (11)$$

$$\Delta H_{\max} = \frac{\Delta\phi}{A \mu_0} \quad (12)$$

$$\Delta M = \frac{\Delta\phi}{A \mu_0} - \Delta H \quad (13)$$

$$H = H_{old} + \Delta H \quad (14)$$

$$M = M_{old} + \Delta M \quad (15)$$

$$\delta = \text{sign}(\Delta H) = \text{sign}(\Delta\phi) \quad (16)$$

Using the values obtained from (14), (15) and (16), the current value of $\frac{dM}{dH}$ is calculated using (9) or (10). A numerical iterative method is used to reduce the error in the calculated value of $\frac{dM}{dH}$ by varying Q .

A. Incorporating losses

The area of the hysteresis loop has an important physical meaning. It represents the amount of energy transformed into heat during one cycle of magnetization. If the area of the loop is measured on the same specimen for different magnetization frequencies f , a substantial increase in the area and change in the shape of the loop can be observed with increasing f .

In the transformer model proposed here, the JA model is used to represent the hysteresis characteristics of the core and hence it properly represents the hysteresis loss of a transformer core. The eddy current effects are incorporated as described below.

A.1 Loss Separation

The concept of loss separation describes the total power loss at a given magnetizing frequency as in (17), where the total losses are divided into three parts, P_{hys} , P_{cls} and P_{exc} . P_{hys} is the hysteresis loss and P_{cls} is known as the classical eddy current loss and is calculated assuming a uniform magnetization. When the calculated values of hysteresis and classical eddy current losses are added, their sum is significantly less than the measured losses. This difference is known as the excess or anomalous losses (P_{exc}) [14].

$$P_{total} = P_{hys} + P_{cls} + P_{exc} \quad (17)$$

Excess loss arises due to the fact that, any ferromagnetic material is made up of self-saturated domains, and hence the microscopic magnetic flux pattern in the material is not smooth and continuous as assumed in calculating the classical eddy current losses. Magnetization proceeds by a movement of domain boundaries and, if the domains are relatively large, the eddy currents induced in the neighborhood of the moving boundaries will differ from the simple classical pattern [13][14].

In the simulation model, the total magnetic field intensity H_{tot} can be expressed as in (18), where H_{hyst} is calculated with the JA model and, the sum of H_{cls} and H_{exc} is added to represent the eddy current effects [16][17].

$$H_{tot} = H_{hyst} + H_{cls} + H_{exc} \quad (18)$$

The instantaneous power loss per unit volume due to classical eddy currents is proportional to the rate of change of magnetization [18]. Thus the energy lost due to classical eddy currents per cycle per unit volume can be represented in the model with an equivalent magnetic field proportional to $\frac{dB}{dt}$. In our model, H_{cls} represents a magnetic field intensity equivalent to the classical eddy current losses. Therefore H_{cls} in (18) can be expressed as $H_{cls} = k_1 \frac{dB}{dt}$, where k_1 is a constant. Similarly the excess energy loss can be represented by an equivalent magnetic field proportional to $(\frac{dB}{dt})^{\frac{1}{2}}$ [15]. Thus H_{exc} in (18) can be expressed as $H_{exc} = k_2 (\frac{dB}{dt})^{\frac{1}{2}}$, where k_2 is a constant. Therefore in the time domain simulations, the total magnetic field intensity H_{tot} can be expressed as

in (19), where k_1 and k_2 are constants for a given transformer. In order to incorporate losses, the magnitude of H calculated in (14) is modified using (19).

$$H_{tot} = H_{hyst} + k_1 \frac{dB}{dt} + k_2 \left(\frac{dB}{dt} \right)^{\frac{1}{2}} \quad (19)$$

B. Calculation of the Current Injections

The calculated H_{tot} value is used to find the branch MMFs. These values are used to calculate the branch permeance P (20). This process is repeated for all the branches in the equivalent circuit that represent a winding or a yoke. Then the branch permeance matrix is updated with the new values of P and the simulation algorithm continues to calculate the magnitudes of the current injected across each winding are calculated using (5), i.e. i_{s1} and i_{s2} .

$$P = \frac{\phi}{MMF} \quad (20)$$

VI. COMPARISON OF SIMULATION AND TEST RESULTS

A series of tests were carried out to validate the new transformer model using a 3kVA, 115V/2300V, 60Hz single phase distribution transformer.

A. Determination of Parameters

The parameters of the JA model using the anhysteretic function represented with (8) were estimated such that the measured saturation characteristic (V_{rms}/I_{rms}) and the recorded waveforms are reasonably accurately produced using the new model.

The numerical determination of the parameters for the anhysteretic magnetization curve from experimental measurements has been presented in [19]. This process has been adopted in [4] to calculate parameters for the current transformer model. The same methodology was used to derive the parameters for the power transformer model presented here. The B-H characteristics of the core material M4 is used for the comparisons with a distribution transformer [20]. The derived parameters are given in the appendix. The slope of the anhysteretic curve in the saturation region and the width of the B-II loop in the shoulder region may be slightly modified to match the characteristics of a given transformer [4].

B. Comparisons with Recorded Waveforms

Simulation results for open circuit tests on a single phase 2 winding transformer model are compared with test results. Simulations were carried out with the electromagnetic transient program PSCAD/EMTDC.

The single-phase two-winding model used has a current source across each winding to represent the saturation. In the new model, the eddy current effects are incorporated into the algorithm before the transformer inductance matrix is calculated. Thus, the calculated value of the saturation current injected across each winding also contains the effects of eddy currents (Fig.5a).

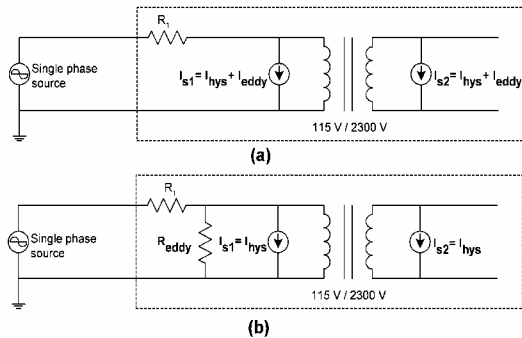


Fig. 5. Simulation models; (a) with the new algorithm, (b) with an external resistor representing losses.

Figure 6 shows the comparison of the simulated waveform and the recorded waveform at the rated voltage and frequency. A close comparison is seen between the simulation and the recorded waveform.

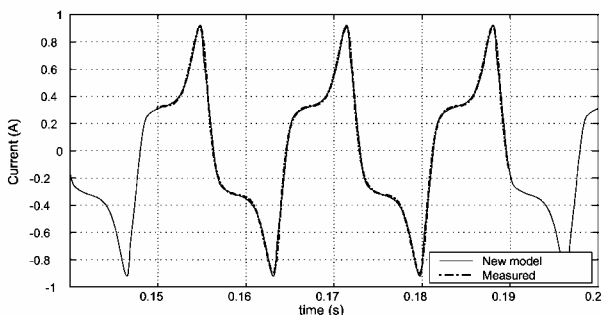


Fig. 6. Magnetizing current at the rated conditions

Simulations were also carried out to compare the new model with a more commonly used approach of representing eddy current losses using a shunt resistor as shown in Fig.(5b). In this ‘resistor model’, hysteresis characteristics are represented by the JA theory, and the eddy current effects are represented with an external resistor connected across the terminals. The magnitude of this resistor is calculated to match the measured core loss at the nominal frequency.

The percentage error in the rms value of the magnetizing current produced by the new model is -1% at the rated conditions. The parameters of the new model were tuned so that an accurate representation is obtained at the rated conditions. Thus the minimum error in the power loss is seen at the rated conditions i.e. 2%. A maximum error of 13% is produced by the new model at 0.9 pu voltage where as, the resistor model produced 11%.

These comparisons show that the resistor model produces a closer match than does the new model. This is due to the fact that the magnitude of the core loss resistor in the resistor model was calculated at 60 Hz and all of the comparisons were carried out at the same frequency. However, the eddy current effects included in the new model are capable of representing the frequency dependency of the B-H characteristics, and the following

comparisons show that it is important to model these effects accurately. Fig.7 shows the comparison of the simulated B-H loops produced with the new model at different excitation frequencies. It shows that the width of the B-H loop increases as the frequency is increased.

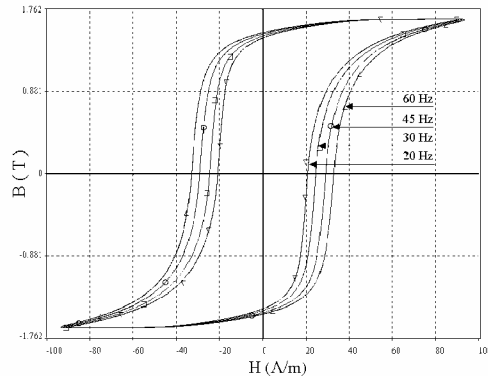


Fig. 7. BH loops at different frequencies

Fig.8a shows the comparison of the core loss at different frequencies. A maximum error of -5% is produced by the new model at 25 Hz where as, the resistor model showed significant deviations with the maximum error of -24% at 25 Hz. Similar observations can be made with the variation of core loss per cycle for frequencies 20 Hz ~ 100 Hz (Fig.8b). Fig.9a and Fig.9b show the comparison of the magnetizing current, and the fundamental component of the magnetizing current at different frequencies.

These comparisons show that the resistor model may cause significant errors as the frequency is decreased. The same trend can be seen when the frequency is increased (70 - 100 Hz). This range could not be verified due to lack of recorded data. However, Fig.8b shows that the new model has a slope much closer to the measured curve and also previous work in this area has indicated a linear variation in this region [13][14]. This confirms that the new model is capable of simulating the magnetizing current and the power losses more accurately than does the commonly used approach of a shunt resistor. In addition, it shows that it is important to model the frequency dependency of the B-H loop. The comparisons at 25Hz are presented in Fig.10.

VII. CONCLUSION

The Jiles-Atherton phenomenological model of a ferromagnetic material has been successfully incorporated into a transformer model of an electromagnetic transient simulation program. The hysteresis model includes the eddy current effects. This representation incorporates losses within the transformer model and hence this algorithm is useful in the simulation of multi-winding transformers. Simulation results for open circuit tests on a single phase 2 winding transformer model are compared

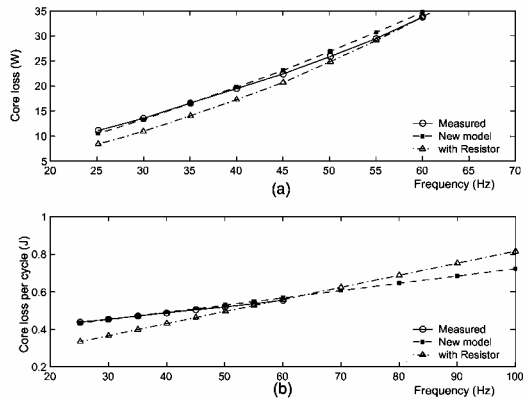


Fig. 8. Comparison of the core loss, and the core loss per cycle at different frequencies

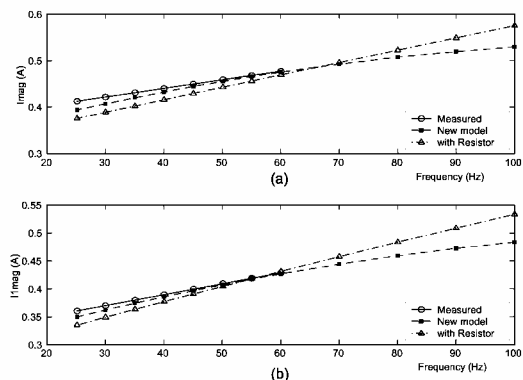


Fig. 9. Comparison of the magnetizing current (I_{mag}) and the fundamental component of I_{mag} at different frequencies

with test results. Simulation results are in good agreement with recorded data.

APPENDIX

Parameters of the hysteresis model;

- $\alpha = 3.90e-6$, $M_{sat} = 1.71e6$, $k = 8.96e-6$, $c = 0.1$, $a_1 = 60$, $a_2 = 96$, and $a_3 = 93$.

Parameters for a given transformer;

- $B_{max} = 1.65$, $A = 2.27$, $l = 0.717$, $k_1 = 3.5e-3$, and $k_2 = 0.79$
- Details of the laboratory test setup are as follows.
- Transformer : 3kVA, 115V/2300V, 60Hz single phase distribution transformer. The magnitude of the external resistor used in Fig.(5b) was calculated at 60Hz, so

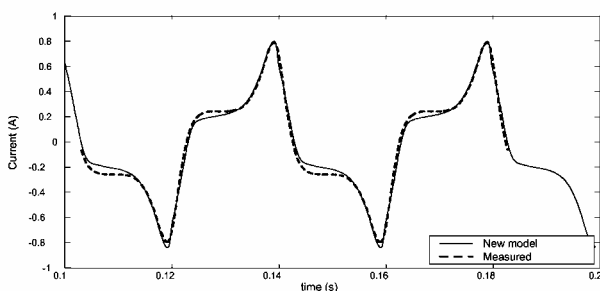


Fig. 10. Magnetizing current at 25Hz, at the rated flux

that the measured power loss is matched; $R_{eddy} = 548\Omega$ referred to 115V.

ACKNOWLEDGMENTS

The Authors are grateful to Manitoba Hydro and the Office of Naval Research (USA) for the financial and technological support to carry out the research described in this paper.

REFERENCES

- [1] F.de Leon, A.Semlyen, "A simple representation of dynamic hysteresis losses in power transformers", *IEEE Trans. Power Delivery*, vol.10, pp. 315-321, Jan. 1995
- [2] F. Liorzou, B. Phelps, and D. L. Atherton, "Macroscopic Models of Magnetization", *IEEE Transactions on Magnetics*, vol. 36, pp.418-428, Mar. 2000
- [3] D.C.Jiles, D.L.Atherton, "Theory of Ferromagnetic Hysteresis", *Journal of Magnetism and Magnetic Materials*, vol. 61, pp. 48-60, 1986
- [4] U.D.Annakkage, P.G.McLaren, E.Dirks, R.P.Jayasinghe and A.D.Parker, "A Current Transformer Model Based on the Jiles-Atherton Theory of Ferromagnetic Hysteresis", *IEEE Transactions on Power Delivery*, vol. 15, pp. 57-61, Jan. 2000
- [5] F.de Leon, A.Semlyen, "Complete transformer model for electromagnetics transients", *IEEE Trans. Power Delivery*, vol.9, pp. 231-239, Jan. 1994
- [6] B.A.Mork, "Five legged wound core transformer model: Derivation, parameters, implementation, and evaluation", *IEEE Transactions on Power Delivery*, vol.14, pp. 1519-1526, Oct. 1999
- [7] X.Chen, "A three phase multi-legged transformer model in ATP using the directly formed inverse inductance matrix", *IEEE Trans. Power Delivery*, vol.11, pp. 1554-1562, July 1996
- [8] C.M.Arturi, "Transient simulation of a three phase five limb step up transformer following an out of phase synchronization", *IEEE Trans. Power Delivery*, vol.6, pp. 196-207, Jan 1991
- [9] T.Fujiwara and R.Tahara, "Eddy current modeling of silicon steel for use on SPICE", *IEEE Trans. Magnetics*, vol.31, pp. 4059-4061, Nov. 1995
- [10] J.Arrillaga, W.Enright, N.R.Watson and A.R.Woods, "Improved simulation of HVDC converter transformers in electromagnetic transient programs", *IEE Proc.-Gener. Transm. Distrib.*, vol.144, pp. 100-106, Mar. 1997
- [11] W.Enright, O.B.Nayak, G.D.Irwin and J.Arrillaga, "An electromagnetic transient model of multi-limb transformers using normalized core concept", in *Proc. International conference on Power Systems Transients (IPST)*, pp. 93-98, Jun. 1997
- [12] Manitoba HVDC Research Centre, "PSCAD/EMTDC User's Guide", 1998
- [13] C.D.Graham, Jr., "Physical origin of losses in conducting ferromagnetic materials", *J.Appl. Phys.*, vol.53, No.11, pp. 8276-8280, Nov. 1982
- [14] G.Bertotti, "General properties of power losses in soft ferromagnetic materials", *IEEE Trans. Magnetics*, vol. 24, No.1, pp. 621-630, Jan. 1988
- [15] D.C.Jiles, "Modelling the effects of eddy current losses on frequency dependent hysteresis in electrically conducting media", *IEEE Trans. Magnetics*, vol. 30, pp. 4326-4328, 1994
- [16] G.Bertotti, "Physical interpretation of eddy current losses in ferromagnetic materials I. Theoretical considerations", *Journal of Applied Physics*, vol. 57, pp. 2110-2117, Mar. 1985
- [17] G.Bertotti, "Physical interpretation of eddy current losses in ferromagnetic materials II. Theoretical considerations", *Journal of Applied Physics*, vol. 57, pp. 2118-2126, Mar. 1985
- [18] S.Chikazumi, *Physics of Magnetism*, John Wiley NY, 1964
- [19] D.C.Jiles, J.B.Tholck and M.K.Devine, "Numerical Determination of Hysteresis Parameters for the modeling of Magnetic Properties Using the Theory of Ferromagnetic Hysteresis", *IEEE Transactions on Magnetics*, vol. 28, pp. 27-35, Jan. 1992
- [20] R.Hasegawa, "Metallic glasses in devices for energy conversion and conservation", *Journal of Non-Crystalline Solids*, vol. 61&62, pp. 725-736, 1984